2021

A Lattice Boltzmann Model for Phase Change Material (PCM) Melting with Porous Media in Heat Exchanger

Dongyu Chen
Center for Environmental Energy Engineering, Department of Mechanical Engineering, University of Maryland, 4164 Glenn Martin Hall Bldg., College Park, MD 20742, United States of America,
dongyuc@umd.edu

Amir Riaz

Vikrant C. Aute

Reinhard Radermacher

A Lattice Boltzmann Model for Phase Change Material (PCM) Melting with Porous Media in Heat Exchanger

Dongyu Chen*, Amir Riaz, Vikrant C. Aute, Reinhard Radermacher

Center for Environmental Energy Engineering (CEEE), Department of Mechanical Engineering, University of Maryland, College Park, MD 20742, United States

* Corresponding Author: dongyuc@umd.edu

ABSTRACT

Phase change material (PCM) is widely used in thermal energy storage systems as it can absorb and release a large amount of heat by the phase change process. Both experimental and numerical studies of PCM have increased substantially in the past two decades. Among them, the phase change in porous media is one of the significant topics. The simulation of PCM melting in porous media is required to characterize the fluid flow and heat transfer behavior, and to provide guidance for the further design and optimization of PCM heat exchangers and thermal energy storage systems. In this paper, a model is developed based on the Lattice Boltzmann method (LBM) to simulate transient phase change in porous media. Double distribution functions coupled with a multi-relaxation-time (MRT) scheme are utilized in LBM for the simulation of the fluid flow and temperature field, respectively. An enthalpy updating scheme is also applied to determine the liquid fraction of PCM, which is used to track the solid-liquid interface. The basic model in Cartesian coordinate is verified with the simulation of PCM phase change in a porous rectangular container. The model is further adapted for use in cylindrical coordinates for simulating the phase change process within porous media in a cylindrical heat exchanger. The developed model is verified by two vertical annulus cases and the results indicate that the developed model can successfully simulate the effects of natural convection and porous media on the thermal flow. More validation cases are expected to be conducted for the developed model to test its ability to simulate the phase change process. And the fully developed model is expected to be applied in a wider field of PCM phase change, which can benefit the design and improvement of PCM heat exchangers in thermal energy storage systems.

1. INTRODUCTION

Thermal energy storage system is one of the useful tools to improve energy efficiency as it can balance the mismatch between energy demand and supply. Generally, there are two types of thermal energy storage systems: sensible heat thermal energy storage (SHTES) system and latent heat thermal energy storage (LHTES) system. LHTES system utilizes phase change material (PCM) to store the energy, which enables the system to absorb and release a large amount of heat with little temperature variation by the phase change process of PCM. Therefore LHTES system has higher energy densities with more stable temperatures during the energy storage process compared with SHTES system. Both experimental and numerical investigations for LHTES system have increased substantially in the past two decades. Most studies have been conducted on the melting or solidification process of the PCM heat exchanger (HX) at the component level (Tay, Bruno, & Belusko, 2012; Caron-Soupart, Fourmigué, Marty, & Couturier, 2016), while a few studies focus on the overall performance at the system level (Bakhshipour, Valipour, & Pahamli, 2017; Qiao, Du, Muehlbauer, Hwang, & Radermacher, 2019; Qiao, Cao, Muehlbauer, Hwang, & Radermacher, 2020). In this paper, numerical simulation is conducted at the component level to reveal the basic physical mechanisms and evaluate the performance of the PCM HX.

Among various numerical methods, the Lattice Boltzmann method (LBM) as a mesoscopic method is an attractive and promising approach to simulate the fluid flow and heat transfer process. Unlike the conventional computation fluid dynamics (CFD) method which solves Navier-Stokes (NS) equations, LBM solves the Boltzmann equations in a discrete form. Moreover, LBM is an explicit method of second-order accuracy with an ability to consider the molecular motions and link them to restore the macroscopic properties. Owing to these features, LBM can have several advantages compared with the conventional CFD method in terms of the computation costs, parallel computing, and the multiphase flow and phase change(Liu, Feng, He, Lu, & Gu, 2019).

Over the past two decades, many Lattice Boltzmann (LB) models have been developed for solid-liquid phase change. Among them, Huang, Wu, and Cheng (2013) developed an enthalpy-based LB model to treat with the latent-heat source term which can avoid the iteration steps in solving energy equations. Liu and He (2015) developed a double multi-relaxation-time (MRT) LB model for PCM melting in porous media at the scale of the representative elementary volume (REV). Gao, Chen, Zhang, and Chen (2017) utilized an enthalpy-based MRT-LB model at the REV scale to simulate transient porous PCM melting with conduction fins. Ren, Meng, and Guo (2018) utilized enthalpy-based immersed boundary LBM to simulate the PCM melting at pore-scale, where the detailed geometry of the porous media was modeled. These studies have laid a solid foundation for investigating PCM phase change with porous media using LBM. However, these models need to be extended to 3D for simulating the convective PCM phase change in cylindrical HX. In that regard, axisymmetric LB model stands out as it simplifies the computation of the thermal flow in cylindrical HX from 3D to 2D, and thereby saves considerable computation costs. In recent years, several axisymmetric LB models were developed for simulating the thermal flow and phase change. For example, D. Li, Ren, Tong, and He (2017) proposed an enthalpy-based axisymmetric LB model for solid-liquid phase change and validated their model by the experimental data from a PCM solidification case. Wang, Liu, and Zhang (2017) developed a non-orthogonal double MRT-LB model for axisymmetric thermal flow with porous media. Liu et al. (2019) further modified this model for simulating incompressible thermal flow. However, some of these axisymmetric models only simulate the porous thermal flow without phase change, while the models that simulate the phase change usually do not consider the porous media. In other words, axisymmetric LB models that consider both porous thermal flow and PCM phase change are limited and need to be further investigated. In this paper, an axisymmetric enthalpy-based double MRT-LB model in REV scale for the porous PCM phase change is developed based on the Cartesian LB model. The Cartesian LB model is first verified with the PCM melting in a porous cavity. Followed by this, the capability of the developed axisymmetric LB model to solve the convective thermal flow with porous media is verified and validated through two vertical annulus cases.

2. MODEL DESCRIPTION

2.1 Macroscopic governing equations

Generally, it is assumed that the fluid flow is laminar and incompressible, both the porous media and the PCM are isotropic and homogeneous, and the viscous heat dissipation is neglected. Specifically for the convective flows with porous media, the Brinkman-Forchheimer extended Darcy approach is utilized to model the momentum equation and account for the non-linearity of the fluid flow within the porous media. And for the energy aspect, the total enthalpy-based energy equation is adopted with the local thermal equilibrium assumption for the PCM melting. Based on the assumptions above, the macroscopic governing equations at the REV scale for axisymmetric convective thermal flows can be determined (D. Li et al., 2017; Liu et al., 2019).

For the PCM phase change in porous media, the fluid flow in the liquid zone is driven by the buoyancy force and the external force exerted by the porous media on the fluid should be considered. According to this, the expression of the total body force $\mathbf{F} = (F_r, F_z)$ is given by (Guo & Zhao, 2002)

$$\mathbf{F} = -\frac{\varphi \nu_l}{K}\mathbf{u} - \frac{\varphi C}{\sqrt{K}}|\mathbf{u}|\mathbf{u} + \varphi \mathbf{G}, \tag{1}$$

where ν_l is the fluid kinematic viscosity, K is the permeability, C is the inertial coefficient which is a function of the geometry of the porous media (Beckermann & Viskanta, 1988a) and $|\mathbf{u}|$ is calculated as $|\mathbf{u}| = \sqrt{u_r^2 + u_z^2}$. The first and second terms on the right-hand side in Eq. (1) represent the first (Darcy's term) and second (Forchheimer's extension) order drag forces between the fluid and the porous structures which are used to account for the effect of the porous media to the fluid flow in the liquid zone. While the third term on the right-hand side in Eq. (1) represents the buoyancy force where the Boussinesq approximation is applied, therefore $\mathbf{G} = (G_r, G_z)$ is given by

$$\mathbf{G} = (0, g\beta(T - T_{ref})), \tag{2}$$

where g is the gravitational acceleration, β is the thermal expansion coefficient and T_{ref} is the reference temperature. Based on the Boussinesq approximation, the density difference due to the temperature variation is combined with the gravitational acceleration for the calculation of the buoyancy force, while this density difference could be ignored for the calculation of other terms in the governing equations under the assumption of the incompressible flow.

The inertial coefficient C is modeled based on the correlated equation (Guo & Zhao, 2002), and the permeability K can be calculated from the Kozeny-Carman equation (Beckermann & Viskanta, 1988a).

The effective thermal diffusivity is defined as $\alpha_e = k_e/(\rho_l c_{p,l})$, where k_e is the effective thermal conductivity, ρ_l and $c_{p,l}$ are the density and specific heat at constant pressure for the pure fluid. The effective thermal conductivity is not only determined by the thermal conductivities of the PCM and the porous media, but also dependent on the structure of the porous media and the volume fraction of the PCM. To evaluate the effective thermal conductivity of the porous PCM, an analytical model based on the tetradecahedron cells is adopted, which was proposed by Yang et al. (2014). Assuming the porosity φ of the porous media is known, the equation to calculate the effective thermal conductivity is given by

$$\frac{k_e}{k_{pm}} = \frac{1-\varphi}{\left(1-e+\frac{3e}{2a}\right)\left[3(1-e)+1.5ae\right]} + \frac{k_l}{k_{pm}}\varphi, \tag{3}$$

where k_{pm} is the thermal conductivity of the porous media, k_l is the thermal conductivity of the liquid PCM, a and e are the two dimensionless parameters which are related to the structure of the porous media. By setting $a = 1.5$ and $e = 0.3$, the results from Yang et. al indicated that the correlated effective thermal conductivity k_e in the high porosity range ($\varphi \geqslant 0.9$) had a good agreement with the experimental data (Yang et al., 2014). Other models developed to describe the effective thermal conductivity were also summarized in Yang et al. (2014), where the models for other porosity ranges could be found.

Several critical dimensionless parameters for the thermal flow at REV scale are defined as follows:

$$Ra = \frac{g\beta(T_h - T_m)L^3}{\nu_l \alpha_l}, Ste = \frac{c_{p,l}(T_h - T_m)}{L_a}, Da = \frac{K}{L^2}, Pr = \frac{\nu_l}{\alpha_l}, Re = \frac{u_c L}{\nu_l}, J = \frac{\nu_e}{\nu_l}, \lambda = \frac{\alpha_e}{\alpha_l}, \tag{4}$$

where the subscript l denotes the properties of the liquid PCM, the subscript e denotes the effective properties, T_h is the highest temperature of the PCM, T_m is the melting temperature of the PCM, L_a is the latent heat of the PCM, L is the characteristic length and u_c is the characteristic velocity which is defined as $u_c = \sqrt{g\beta(T_h - T_m)L}$ for the convective thermal flow. The listed dimensionless parameters in Eq. (4) are the Rayleigh number Ra, the Stefan number Ste,the Darcy number Da,the Prandtl number Pr,the Reynolds number Re, the viscosity ratio J and the thermal diffusivity ratio λ respectively.

2.2 Enthalpy equations

Under the local thermal equilibrium assumption, the local temperatures among the liquid PCM, the solid PCM and the porous media remain the same. Thereby the local temperature is represented as T for all the components. The corresponding enthalpy h can be then divided into the sensible entalpy and the latent enthalpy ($h = h_{sensible} + h_{latent}$). The general method followed in LB models to describe enthalpy is by defining the enthalpy h as a linear funciton of the temperature and the liquid fraction of the PCM. Based on this method, the sensible enthalpy and the latent enthalpy can be expressed as

$$h_{sensible} = \varphi\left[f_l c_{p,l} + (1-f_l)\frac{\rho_s}{\rho_l}c_{p,s}\right]T + (1-\varphi)\frac{\rho_{pm}}{\rho_l}c_{p,pm}T, \tag{5}$$

$$h_{latent} = \varphi f_l L_a, \tag{6}$$

where $c_{p,s}$ and $c_{p,pm}$ are the specific heat at constant pressure for the solid PCM and the porous media respectively, ρ_s and ρ_{pm} are the mean densities of the solid PCM and the porous media respectively and f_l is the liquid fraction of the PCM defined as,

$$f_l = \begin{cases} 0, & h \leqslant h_s, \\ \frac{h-h_s}{h_l-h_s}, & h_s < h < h_l, \\ 1, & h \geqslant h_l, \end{cases} \tag{7}$$

where h_s is the enthalpy at the temperature T_s when the PCM starts to melt, and h_l is the enthalpy at the temperature T_l when the PCM fully turns into liquid. The difference between T_s and T_l is also known as the temperature glide of the PCM ($\Delta T_{glide} = T_l - T_s$).

2.3 Axisymmetric MRT-LB model for velocity field

In this model, the velocity field of the PCM is only calculated and updated in liquid region. Thereby the MRT-LB equation for axisymmetric porous flow in REV scale can be adopted to describe the motion of the liquid PCM without considering the solid region, and the general form of the equation based on the D2Q9 lattice is given by (Liu et al., 2019)

$$\mathbf{f}(\mathbf{x}+\mathbf{e}\delta_t, t+\delta_t) - \mathbf{f}(\mathbf{x},t) = -\mathbf{M}^{-1}\mathbf{S}\left[\mathbf{m}(\mathbf{x},t) - \mathbf{m}^{eq}(\mathbf{x},t)\right] + \delta_t \mathbf{M}^{-1}\left(\mathbf{I} - \frac{\mathbf{S}}{2}\right)\mathbf{F}_m, \tag{8}$$

where $\mathbf{f}(\mathbf{x},t)$ is the vector of the density distribution functions at given location $\mathbf{x} = (r,z)$ and time t, $\mathbf{e}$ is the vector of the discrete velocities, $\mathbf{M}$ is the transition matrix, $\mathbf{S}$ is the relaxation matrix, $\mathbf{m}(\mathbf{x},t)$ and $\mathbf{m}^{eq}(\mathbf{x},t)$ are the moment vector and the corresponding equilibrium moment vector respectively , $\mathbf{I}$ is the identity matrix, $\mathbf{F}_m$ is the forcing term in the moment space and δ_t is the discrete time step.

For the D2Q9 lattice, the vector of the discrete velocities $\mathbf{e}$ is defined as

$$\mathbf{e} = \{e_i | i = 0, 1, ..., 8\}, \tag{9}$$

where $e_i = (e_{ir}, e_{iz})$ is given by

$$e_i = c[(0,0),(1,0),(0,1),(-1,0),(0,1),(1,1),(-1,1),(-1,-1),(1,-1)]^T, \tag{10}$$

where $c = \delta_r/\delta_t$ is the lattice speed and δ_r is the discrete lattice spacing in the r direction.

The transition matrix $\mathbf{M}$ in non-orthogonal form for D2Q9 lattice can be found in Liu, He, Li, and Li (2016). Followed by this, equilibrium moment vector $\mathbf{m}^{eq}$ for the corresponding moment vector $\mathbf{m}$ can be calculated by

$$\mathbf{m}^{eq} = \mathbf{M}\mathbf{f}^{eq} = r\left[\rho, j_r, j_z, e^{eq}, p_{rr}^{eq}, p_{rz}^{eq}, q_r^{eq}, q_z^{eq}, \varepsilon^{eq}\right]^T, \tag{11}$$

where

$$j_r = \rho_0 u_r,\ j_z = \rho_0 u_z,\ e^{eq} = -2\rho + \frac{3\rho_0(u_r^2+u_z^2)}{\varphi},\ p_{rr}^{eq} = \frac{\rho_0(u_r^2-u_z^2)}{\varphi},\ p_{rz}^{eq} = \frac{\rho_0 u_r u_z}{\varphi},$$
$$q_r^{eq} = -\rho_0 u_r,\ q_z^{eq} = -\rho_0 u_z,\ \varepsilon^{eq} = \rho - \frac{3\rho_0(u_r^2+u_z^2)}{\varphi}, \tag{12}$$

and the vector of the equilibrium distribution functions $\mathbf{f}^{eq} = \{f_i^{eq} | i = 0, 1, ..., 8\}$ in velocity space is given by

$$f_i^{eq} = \omega_i r\rho + \omega_i r\rho_0\left[\frac{\mathbf{e}_i\cdot\mathbf{u}}{c_s^2} + \frac{(\mathbf{e}_i\cdot\mathbf{u})^2}{2\varphi c_s^4} - \frac{|\mathbf{u}|^2}{2\varphi c_s^2}\right], \tag{13}$$

where $c_s = c/\sqrt{3}$ is the lattice sound speed of the D2Q9 model, and ω_i is the weight coefficient of the D2Q9 model (Liu et al., 2016).

Based on the moment vector given in Eq. (11), the relaxation matrix $\mathbf{S}$ can be determined as

$$\mathbf{S} = diag(s_\rho, s_j, s_j, s_e, s_v, s_v, s_q, s_q, s_\varepsilon), \tag{14}$$

where overall the components of the relaxation matrix $s_i \in (0,2)$. Among them, $s_\rho = s_j = 1.0$ indicates the mass and momentum are conserved in the flow region, and the critical relaxation rate s_v, which determines the flow pattern, is related to the fluid viscosity and can be expressed as

$$s_v = \frac{1}{\frac{v_e}{c_s^2\delta_t} + 0.5}, \tag{15}$$

where v_e is the effective kinematic viscosity.

The forcing term $\mathbf{F}_m$ in the moment space is then defined as (Wang et al., 2017)

$$\mathbf{F}_m = \frac{1}{3}r\rho_0\begin{bmatrix} 0 \\ 3\tilde{F}_r \\ 3\tilde{F}_z \\ 6(u_r\tilde{F}_r + u_z\tilde{F}_z)/\varphi \\ 6(u_r\tilde{F}_r - u_z\tilde{F}_z)/\varphi \\ 3(u_r\tilde{F}_z + u_z\tilde{F}_r)/\varphi \\ \tilde{F}_r \\ \tilde{F}_z \\ 2(u_r\tilde{F}_z + u_z\tilde{F}_r)/\varphi \end{bmatrix}, \tag{16}$$

where $\tilde{F}_r = F_r + \frac{c_s^2}{r}\left[1 - \frac{2(s_v^{-1}-0.5)u_r}{r}\right]$ and $\tilde{F}_z = F_z$ are the modified components of the total body force **F**, where F_r and F_z are determined by Eq. (1).

The macroscopic fluid density ρ and velocity $\mathbf{u} = (u_r, u_z)$ can be recovered from the density distribution functions f_i (Guo & Zhao, 2002), as given below:

$$\rho = \frac{1}{r}\sum_{i=0}^{8} f_i, \tag{17}$$

$$\mathbf{u} = \frac{\mathbf{v}}{\mathbf{d}_0 + \sqrt{\mathbf{d}_0^2 + d_1|\mathbf{v}|}}, \tag{18}$$

where $\mathbf{d}_0 = (d_{0r}, d_{0z})$ and d_1 can be determined through the method introduced in Liu et al. (2016).

2.4 Axisymmetric MRT-LB model for temperature field

A D2Q9 MRT-LB thermal model based on the enthalpy method (D. Li et al., 2017) is adopted to simulate the convective heat transfer within porous media. To be consistent with Eq. (8) from the MRT-LB model for the velocity field, the general thermal LB equation is given by

$$\mathbf{g}(\mathbf{x} + \mathbf{e}\delta_t, t + \delta_t) - \mathbf{g}(\mathbf{x}, t) = -\mathbf{N}^{-1}\mathbf{R}\left[\mathbf{n}(\mathbf{x}, t) - \mathbf{n}^{eq}(\mathbf{x}, t)\right] + \delta_t\mathbf{N}^{-1}\mathbf{Q}_m, \tag{19}$$

where $\mathbf{g}(\mathbf{x}, t)$ is the vector of the enthalpy distribution functions, $\mathbf{n}(\mathbf{x}, t)$ and $\mathbf{n}^{eq}(\mathbf{x}, t)$ are the moment vector and the equilibrium moment vector corresponding to $\mathbf{g}(\mathbf{x}, t)$ respectively and $\mathbf{Q}_m$ is the source term in the moment space.

For D2Q9 lattice, the vector of the discrete velocities **e** is defined in the same way as Eqs. (9) and (10) in Section 2.3, while the transition matrix **N** can be found in D. Li et al. (2017), and the corresponding relaxation matrix **R** is then defined as

$$\mathbf{R} = diag(\sigma_h, \sigma_e, \sigma_\varepsilon, \sigma_j, \sigma_q, \sigma_j, \sigma_q, \sigma_p, \sigma_p). \tag{20}$$

According to the definitions of the vector of the entahply distribution functions $\mathbf{g} = \{g_i | i = 0, 1, ..., 8\}$ and the moment vector $\mathbf{n} = \mathbf{N}[g_0, g_1, ..., g_8]^T$, the equilibrium moment vector $\mathbf{n}^{eq}$ is given as

$$\begin{aligned}\mathbf{n}^{eq} = \mathbf{N}\mathbf{g}^{eq} = \Bigg[&h, -4h + 2c_{p,ref}T + \frac{3c_pT|\mathbf{u}|^2}{c^2}, 4h - 3c_{p,ref}T - \frac{3c_pT|\mathbf{u}|^2}{c^2},\\ &\frac{c_pTu_r}{c}, -\frac{c_pTu_r}{c}, \frac{c_pTu_z}{c}, -\frac{c_pTu_z}{c}, \frac{c_pT(u_r^2 - u_z^2)}{c^2}, \frac{c_pTu_ru_z}{c^2}\Bigg],\end{aligned} \tag{21}$$

where $c_{p,ref}$ is a reference specific heat which can be set as $c_{p,ref} = 2c_{p,s}c_{p,l}/(c_{p,s} + c_{p,l})$, and the vector of the equilibrium distribution functions $\mathbf{g}^{eq} = \{g_i^{eq} | i = 0, 1, ..., 8\}$ is given by

$$g = \begin{cases} h - c_{p,ref}T + \omega_i c_{p,ref}T - \omega_i c_pT\dfrac{|\mathbf{u}|^2}{2c_s^2}, & i = 0, \\ \omega_i c_{p,ref}T + \omega_i c_pT\left[\dfrac{(\mathbf{e}_i \cdot \mathbf{u})}{c_s^2} + \dfrac{(\mathbf{e}_i \cdot \mathbf{u})^2}{2c_s^4} - \dfrac{|\mathbf{u}|^2}{2c_s^2}\right], & i \neq 0. \end{cases} \tag{22}$$

The source term $\mathbf{Q}_m$ can then be determined as

$$\mathbf{Q_m} = \left[-\frac{c_pTu_r}{r}, 0, 0, 0, 0, 0, 0, 0, 0\right], \tag{23}$$

and to recover the macroscopic governing equation, the first component of the redistributed moment vector n_0^* after the collision process can be modified, as shown below:

$$n_{0,new}^* = n_0^* - \frac{1}{r}(1 - 0.5\sigma_j)c\delta_t(n_3 - n_3^{eq}), \tag{24}$$

The enthalpy h can be simply calculated as

$$h = \sum_{i=0}^{8} g_i, \tag{25}$$

and the corresponding temperature and liquid fraction can be calculated by Eq. (7) in Section 2.2.

3. NUMERICAL SIMULATIONS

In this section, a simulation of the PCM melting in a porous square cavity is conducted to test the performance of the basic Cartesian LB model. The square cavity is shown in Fig. 1, where the left plate is kept at the highest temperature T_h = 45 °C and the right plate is kept at the lowest temperature T_c = 20 °C. Additionally, both the top and bottom plate are adiabatic and this porous cavity is filled with the solid PCM initially. The melting temperature of the PCM T_m = 29.78 °C and the initial temperature $T_i = T_c$, thereby the solid PCM starts to melt from the left side to the right side as time continues. To compare with the results of the LBM simulation from Liu and He (2015), the computational domain is set to $[N_x, N_y] = [200, 200]$ and other parametric settings are listed in Table 1.

The temperature profile at Fourier Number $Fo = \alpha t/L^2 = 1.829$ is shown in Fig. 2, where $\theta = (T - T_c)/(T_h - T_c)$ is the dimensionless temperature, the lines are the results from the present model and the dots are the numerical data points from Beckermann and Viskanta (1988b). The comparison shows a good agreement and indicates that the basic Cartesian LB model is capable of solving the convective PCM melting with the porous media.

Table 1: Dimensionless Number for the PCM melting in the porous cavity

Rayleigh Number	Prandtl Number	Stefan Number	Porosity
841,000	0.0208	0.1241	0.385

The axisymmetric LB model developed based on the Cartesian LB model is then utilized to simulate two cases of the thermal flow in a vertical annulus, as shown in Fig. 3. The purpose of these two cases is to verify and validate the ability of the present axisymmetric model to solve the thermal flow with natural convection. The two cases are as follows:

1. Case one is the thermal flow without porous media at variant Rayleigh numbers ($Ra = 10^3,\ 10^4,\ 10^5$), where the computational domain is $[N_r, N_z] = [100, 200]$ and both the aspect ratio $L/(r_o - r_i)$ and the diameter ratio r_o/r_i are set to 2. The highest temperature T_h is kept at 60 °C and lowest temperature T_c is 50 °C. The isotherms for different Ra are displayed in Fig. 4 and the corresponding average Nusselt numbers are tabulated in Table 2 in comparison with other numerical results.
2. Case two is the thermal flow with the porous media. The temperature settings are the same with the case one and the rest of the settings is listed in Table 3. The simulation results are shown in Fig. 5 in comparison with the experimental data from Prasad and Kulacki (1985).

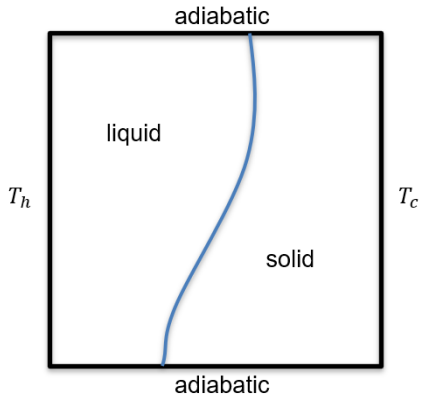

Figure 1: Porous square cavity with PCM

Table 2: Comparison of the average Nusselt numbers

Ra	L. Li, Mei, and Klausner (2013)	Wang, Zhang, and Zhang (2016)	Present model
10^3	1.692	1.688	1.685
10^4	3.215	3.210	3.207
10^5	5.787	7.795	5.741

Table 3: Dimensionless Number for the PCM melting in the porous annulus

Aspect ratio	Diameter ratio	Porosity	Da	Ra	Pr
2.0	5.338	0.3698	1.66×10^{-6}	1.75×10^{8}	1.0

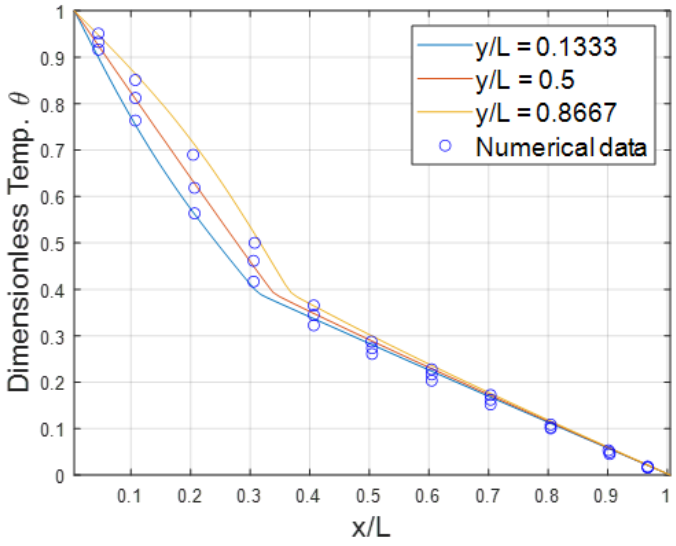

Figure 2: Temperature profile of PCM melting in the porous cavity at Fo = 1.829

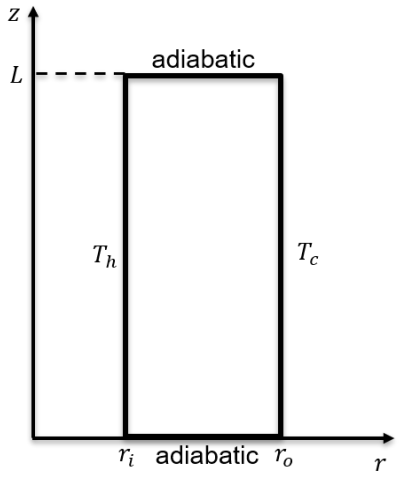

Figure 3: The cross-section area of the vertical annulus

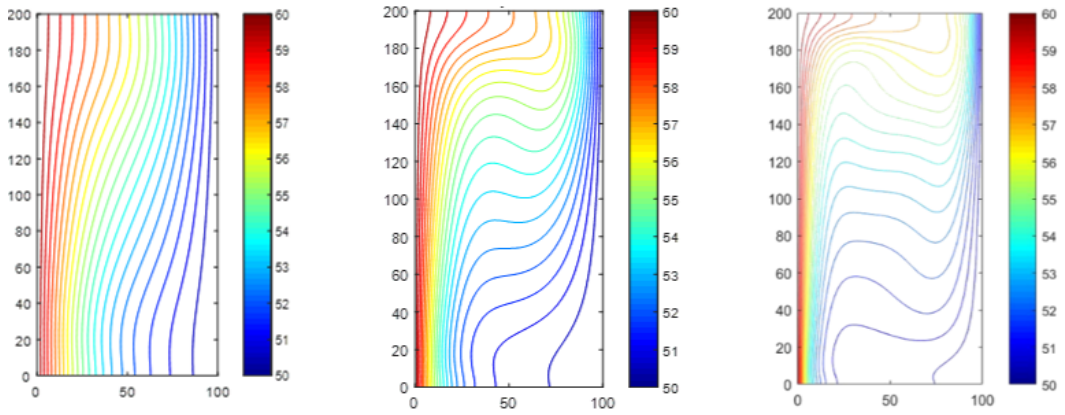

Figure 4: Isotherms (units: °C) of the thermal flow in the annulus for $Ra = 10^3$ (left), 10^4 (middle), 10^5 (right)

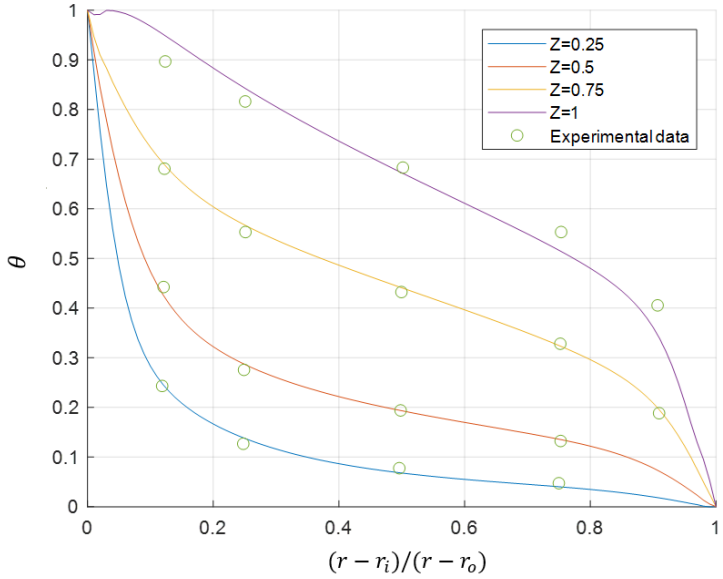

Figure 5: Temperature profile of the thermal flow in the porous annulus along radius at different height $Z = z/L$

4. CONCLUSIONS

A Lattice Boltzmann model has been developed for PCM melting with the porous media. The basic Cartesian LB model is verified with the PCM melting in a porous square cavity and the developed axisymmetric LB model is verified and validated with two cases of the thermal flow in a vertical annulus. For case one, a clear trend can be seen in Fig. 4 that more hot fluid is driven from the bottom to the top near the inner plate as the Rayleigh number becomes higher, which results in the different temperature distributions. Moreover, the comparison of the average Nusslet numbers indicates that the present axisymmetric model is capable of solving thermal flow with natural convection. For case two, the porous media is considered in the convective thermal flow. The comparison with the experimental data in Fig. 5 shows that the present model can handle the thermal flow with the porous media accurately. The developed model in this paper still needs to be validated with the experimental data of the PCM melting in cylindrical HX to further prove its capability in solving the phase change process at axisymmetric coordinates. More cases such as the PCM melting with circular fins and the PCM solidification in HX are expected to be investigated by the developed model in the future.

NOMENCLATURE

LBM	Lattice Boltzmann method	(-)	k	conductivity	(W/(m·K))
LB	Lattice Boltzmann	(-)	Ra	Rayleigh number	(-)
HX	heat exchanger	(-)	Ste	Stefan number	(-)
PCM	phase change material	(-)	Da	Darcy number	(-)
CFD	computational fluid dynamics	(-)	Pr	Prandtl number	(-)
			J	viscosity ratio	(-)
SHTES	sensible heat thermal energy storage	(-)	λ	thermal diffusivity ratio	(-)
			h	enthalpy	(kJ/kg)
LHTES	latent heat thermal energy storage	(-)	L_a	latent heat	(kJ/kg)
			f_l	liquid fraction	(-)
φ	porosity	(-)	ω_i	weight coefficient	(-)
T	temperature	(°C)	M	non-orthogonal transition matrix	(-)
θ	dimensionless temperature	(-)			
L	characteristic length	(-)	N	transition matrix	(-)
u	velocity	(m/s)	c	lattice speed	(-)
u_c	characteristic velocity	(-)	$\mathbf{f}$	density distribution function	(-)
c_p	specific heat at constant pressure	(kJ/(kg·K))	$\mathbf{m}$	moment vector for velocity field	(-)
C	inertial coefficient	(-)			
K	permeability	(-)	$\mathbf{g}$	temperature distribution function	(-)
v	viscosity	(Pa·s)			
α	thermal diffusivity	(m^2/s)	$\mathbf{n}$	moment vector for temperature field	(-)
β	thermal expansion coefficient	(K^{-1})	$\mathbf{e}$	discrete lattice velocities	(-)
g	gravitational acceleration	(m/s^2)	$\mathbf{Q}_m$	source term	(-)
d_p	mean diameter of porous media	(m)	$\mathbf{F}$	total body force	(N)
			$\mathbf{G}$	buoyancy force	(N)

Subscript

r	radius
z	height
l	liquid
s	solid
e	effective
ref	reference
h	hot
c	cold
m	melting
pm	porous media

REFERENCES

Bakhshipour, S., Valipour, M. S., & Pahamli, Y. (2017). Analyse paramétrique de réfrigérateurs domestiques utilisant un échangeur de chaleur à matériau à changement de phase. *International Journal of Refrigeration*, *83*, 1–13. doi: 10.1016/j.ijrefrig.2017.07.014

Beckermann, C., & Viskanta, R. (1988a). Natural convection solid/liquid phase change in porous media. *International Journal of Heat and Mass Transfer*, *31*(1), 35–46. doi: 10.1016/0017-9310(88)90220-7

Beckermann, C., & Viskanta, R. (1988b). Natural convection solid/liquid phase change in porous media. *International Journal of Heat and Mass Transfer*, *31*(1), 35 - 46. doi: https://doi.org/10.1016/0017-9310(88)90220-7

Caron-Soupart, A., Fourmigué, J. F., Marty, P., & Couturier, R. (2016). Performance analysis of thermal energy storage systems using phase change material. *Applied Thermal Engineering*, *98*, 1286–1296. doi: 10.1016/j.applthermaleng.2016.01.016

Gao, D., Chen, Z., Zhang, D., & Chen, L. (2017). Lattice Boltzmann modeling of melting of phase change materials in porous media with conducting fins. *Applied Thermal Engineering*, *118*, 315–327. doi: 10.1016/j.applthermaleng .2017.03.002

Guo, Z., & Zhao, T. S. (2002). Lattice Boltzmann model for incompressible flows through porous media. *Physical Review E - Statistical Physics, Plasmas, Fluids, and Related Interdisciplinary Topics*, *66*(3), 1–9. doi: 10.1103/ PhysRevE.66.036304

Huang, R., Wu, H., & Cheng, P. (2013). A new lattice Boltzmann model for solid-liquid phase change. *International Journal of Heat and Mass Transfer*, *59*(1), 295–301. doi: 10.1016/j.ijheatmasstransfer.2012.12.027

Li, D., Ren, Q., Tong, Z. X., & He, Y. L. (2017). Lattice Boltzmann models for axisymmetric solid–liquid phase change. *International Journal of Heat and Mass Transfer*, *112*, 795–804. doi: 10.1016/j.ijheatmasstransfer.2017.03.127

Li, L., Mei, R., & Klausner, J. F. (2013). Multiple-relaxation-time lattice boltzmann model for the axisymmetric convection diffusion equation. *International Journal of Heat and Mass Transfer*, *67*, 338 - 351. doi: https:// doi.org/10.1016/j.ijheatmasstransfer.2013.08.039

Liu, Q., Feng, X. B., He, Y. L., Lu, C. W., & Gu, Q. H. (2019). Multiple-relaxation-time lattice Boltzmann model for simulating axisymmetric thermal flows in porous media. *International Journal of Heat and Mass Transfer*, *137*, 1301–1311. doi: 10.1016/j.ijheatmasstransfer.2019.03.118

Liu, Q., & He, Y. L. (2015). Double multiple-relaxation-time lattice Boltzmann model for solid-liquid phase change with natural convection in porous media. *Physica A: Statistical Mechanics and its Applications*, *438*, 94–106. doi: 10.1016/j.physa.2015.06.018

Liu, Q., He, Y. L., Li, D., & Li, Q. (2016). Non-orthogonal multiple-relaxation-time lattice Boltzmann method for incompressible thermal flows. *International Journal of Heat and Mass Transfer*, *102*, 1334–1344. doi: 10.1016/ j.ijheatmasstransfer.2016.06.029

Prasad, V., & Kulacki, F. A. (1985, 02). Natural Convection in Porous Media Bounded by Short Concentric Vertical Cylinders. *Journal of Heat Transfer*, *107*(1), 147-154. doi: 10.1115/1.3247371

Qiao, Y., Cao, T., Muehlbauer, J., Hwang, Y., & Radermacher, R. (2020). Experimental study of a personal cooling system integrated with phase change material. *Applied Thermal Engineering*, *170*(October 2019), 115026. doi: 10.1016/j.applthermaleng.2020.115026

Qiao, Y., Du, Y., Muehlbauer, J., Hwang, Y., & Radermacher, R. (2019). Experimental study of enhanced PCM exchangers applied in a thermal energy storage system for personal cooling. *International Journal of Refrigeration*, *102*, 22–34. doi: 10.1016/j.ijrefrig.2019.03.006

Ren, Q., Meng, F., & Guo, P. (2018). A comparative study of PCM melting process in a heat pipe-assisted LHTES unit enhanced with nanoparticles and metal foams by immersed boundary-lattice Boltzmann method at pore-scale. *International Journal of Heat and Mass Transfer*, *121*, 1214–1228. doi: 10.1016/j.ijheatmasstransfer.2018.01 .046

Tay, N. H., Bruno, F., & Belusko, M. (2012). Experimental validation of a CFD model for tubes in a phase change thermal energy storage system. *International Journal of Heat and Mass Transfer*, *55*(4), 574–585. doi: 10.1016/ j.ijheatmasstransfer.2011.10.054

Wang, Z., Liu, Y., & Zhang, J. (2017). Double MRT lattice Boltzmann model for axisymmetric convective flow in porous media. *International Journal of Heat and Mass Transfer*, *112*, 810–813. doi: 10.1016/ j.ijheatmasstransfer.2017.04.053

Wang, Z., Zhang, W., & Zhang, J. (2016). Lattice boltzmann simulations of axisymmetric natural convection with anisotropic thermal diffusion. *International Journal of Heat and Mass Transfer*, *101*, 1304 - 1315. doi: https:// doi.org/10.1016/j.ijheatmasstransfer.2016.05.002

Yang, X. H., Bai, J. X., Yan, H. B., Kuang, J. J., Lu, T. J., & Kim, T. (2014). An Analytical Unit Cell Model for the Effective Thermal Conductivity of High Porosity Open-Cell Metal Foams. *Transport in Porous Media*, *102*(3), 403–426. doi: 10.1007/s11242-014-0281-z